

Submitted to ApJ Letters

## Effective Radii and Color Gradients in Radio Galaxies

Ashish Mahabal<sup>1</sup> and Ajit Kembhavi

Inter-University Centre for Astronomy and Astrophysics, Post Bag 4, Ganeshkhind,  
Pune 411 007, India

and

P. J. McCarthy

Observatories of the Carnegie Institute of Washington, Pasadena, CA, USA

### ABSTRACT

We present de Vaucouleurs' effective radii in  $B$  and  $R$  bands for a sample of MRC radio galaxies and a control sample of normal galaxies. We use the ratio of the scale lengths in the two bands as an indicator to show that the radio galaxies tend to have excess of blue color in their inner region much more frequently than the control galaxies. We show that the scale length ratio is a useful indicator of radial color variation even when the conventional color gradient is too noisy to serve the purpose. We also discuss other interesting morphological features of radio galaxies including departures from de Vaucouleurs' law profiles in their central regions.

*Subject headings:* galaxies: active — galaxies: structure

### 1. Introduction

Traditionally, radio galaxies were believed to be ellipticals consisting of a coeval population of old stars, and almost no dust or gas. However, detailed photometric studies in the optical band, as well as X-ray observations, have demonstrated that elliptical galaxies, especially those hosting radio sources, not only have significant quantities of dust and gas, but also possess fine structure indicating some amount of activity in the past  $\sim 10^2$  million years (see e.g. Smith and Heckman 1989). Radio galaxies host an active galactic nucleus (AGN) and also have radio jets which transport a very large amount of energy over hundreds of kiloparsecs. Such phenomena are likely to be associated with morphological features not found in normal elliptical galaxies.

---

<sup>1</sup>present address: Physical Research Laboratory, A and A division, Navrangpura, Ahmedabad, India

In this paper we present the main results from a detailed morphological study of a sample of radio galaxies from the *Molonglo Reference Catalogue* (MRC). We present de Vaucouleurs' effective radii (scale lengths), obtained from careful model fits to surface brightness profiles of the galaxies, and show that the ratio  $r_e(B)/r_e(R)$ , of the scale lengths in  $B$  and  $R$  filters, provides a measure of the color gradient in the galaxy. The ratio is related to color gradients measured conventionally, but is more robust: it can provide an estimate of the color gradient even when the signal-to-noise ratio is not good enough for the color gradient to be measured unambiguously using the conventional technique. Using the ratio we show that a large fraction of radio galaxies become bluer towards the center.

Our model fits indicate that several radio galaxies have a significant disk-like structure. The radio galaxies tend to deviate, near the center, from fitted model profiles more often than control galaxies. We argue that in addition to possible genuine departures from de Vaucouleurs' law the central deviations indicate excess emission or dust absorption in the region.

## 2. Sample and observations

Our results are based on the observations of 30 galaxies from the MRC which have 408 MHz radio flux  $S_{408} > 0.95$  Jy, redshift  $z < 0.3$  and  $-30 \text{ deg} \leq \delta(1950) \leq -20 \text{ deg}$ . The objects were observed from the Las Campanas Observatory (LCO), Chile in Jan 1995 and Feb 1996 using the 1.0m f/7 Swope telescope and the 2.5m f/7.5 Du Pont telescope. Images were obtained in Johnson's  $B$  and Cousin's  $R$  filters, which are centered at  $0.44\mu\text{m}$  and  $0.65\mu\text{m}$  respectively and have a bandwidth of  $\sim 0.1\mu\text{m}$ . The typical exposure time was  $\sim 20$  min in  $R$  and  $\sim 60$  min in  $B$ . All the processing was done in the normal way using tasks from IRAF and STSDAS, and the details will be published elsewhere (Mahabal et al. 1998a).

For the purpose of comparison we extracted a control sample from the CCD fields of our radio galaxies. The sample consists of all non-radio, early type galaxies from the fields which have semi-major axis length  $> 15''$ . There are 30 galaxies in the sample, and these were processed and analyzed in a fashion identical to the radio galaxies.

## 3. Surface photometry

We fitted the isophotes of each galaxy in both  $B$  and  $R$  filters with a succession of ellipses with different semi-major axis lengths using tasks in IRAF based on the algorithm described by Jedrzejewski (1987). The mean brightness for the series of best-fit ellipses gives us the radial brightness profile of a galaxy as a function of semi-major axis length. From the radial profile in the two bands we obtained the  $B - R$  color profile for each galaxy.

Major contributions to the galaxian light can in general come from a spheroidal bulge

supported by random velocities of stars and having small rotation and from a flattened disk rotating about an axis perpendicular to it. In active galaxies an additional substantial contribution to the central region can be made by the active galactic nucleus (AGN) acting as a point source. The relative strengths of the components vary over galaxy type, and can be determined by fitting the observed radial brightness profile of the galaxy with a composite model made up of contributions from each component.

We have assumed that the bulge profile is described by de Vaucouleurs' law, and the disk profile by an exponential. The contribution of the AGN corresponds to a point source broadened by the point spread function. We have found for our sample of radio galaxies that the AGN is too weak to be unambiguously detected, and distinguished from other compact features which may be present, with our data. We therefore do not include an AGN in our fits. The model surface brightness  $I(r)$  at semi-major axis length  $r$  is then given by

$$I(r) = I_e \exp\{-7.67[(r/r_e)^{1/4} - 1]\} + I_d \exp(-r/r_d) \quad (1)$$

where  $I_e$  is the bulge intensity at de Vaucouleurs' effective radius (scale length)  $r_e$ ,  $I_d$  is the disk brightness at  $r = 0$ , and  $r_d$  is the disk scale-length.

We have tried fitting just a bulge (B), as well as a bulge and a disk (B+D) to our galaxies. We find on the whole that the B+D combination is the best overall, and our analysis is based on that combination. In most radio galaxies the disk component turns out to be negligible or quite small, which is consistent with radio galaxies being largely of the early type.

To obtain the best-fit model to an observed galaxy profile, we generate a model galaxy with two dimensional surface brightness distribution corresponding to trial values of the four parameters in Equation 1, and observe bulge and disk ellipticities. We convolve the model with a Gaussian point-spread function (PSF) determined from the observed frames for the galaxy in question, and then obtain the model radial profile. We determine the best-fit parameters by minimizing reduced chi-square function  $\chi_\nu^2 = \sum(I_o - I_m)^2/\sigma^2$ , where  $I_o$  and  $I_m$  are the observed and model surface brightnesses at specific distances along the semi-major axis. The standard deviation  $\sigma$  at each point is obtained from the ellipse fitting task in IRAF and includes photon counting as well as ellipse fitting errors. Contributions to  $\chi_\nu^2$  are obtained at semi-major axis lengths  $r$  in the range  $r_1 < r < r_2$ , where the inner limit  $r_1$  is chosen such that it lies at a radial separation of 1.5 times the full width at half maximum (FWHM) of the PSF. The outer limit  $r_2$  is chosen to be where  $\sigma(I)/I$  drops to 0.1.

## 4. Results of profile fits

### 4.1. Goodness of fit

We get very good ( $\chi_\nu^2 < 1$ ) or acceptable ( $1 < \chi_\nu^2 < 2$ ) fits in  $\sim 85\%$  of the cases for the radio as well as the control sample. It follows that strong radio sources *do not* prefer highly distorted

galaxies.  $\chi_\nu^2$  does not increase as a function of redshift i. e., we get good fits right upto the redshift of 0.3 that we have considered. (See Figure 1). We find that  $\chi_\nu^2(B)$  values are in general smaller than the corresponding  $\chi_\nu^2(R)$  values. The lower values in  $B$  are partly due to the higher  $\sigma$  values there. It also appears that isophote distorting influences like emission and absorption regions which could increase  $\chi_\nu^2(B)$  are averaged out in the ellipse and profile fits. The distribution of  $\chi_\nu^2$  values is shown in Figure 1

#### 4.2. Disk parameters

The profile fits show that half the radio galaxies in our sample have disk component with disk-to-bulge luminosity ratio  $D/B > 0.1$ . The fraction of such  $D/B$  values is just a bit higher for the control sample. Values of  $D/B < 0.1$  are not taken to be significant in our data. About half the galaxies with  $D/B > 0.1$  have disk scale lengths  $r_d$  smaller than the FWHM of the PSF, for the radio as well as the control sample. In galaxies with  $D/B > 0.1$ ,  $r_d$  exceeding the FWHM we find that  $r_d(B) \approx r_d(R)$  and (2)  $(D/B)_{blue} \approx (D/B)_{red}$ . There are several radio galaxies with  $D/B > 0.3$ , which puts them in the class of lenticulars or early type spirals. We will discuss these cases further in a separate publication (Mahabal et al., 1998b, in preparation).

#### 4.3. Bulge parameters

We now turn to the bulge scale lengths. Figure 2 shows a plot of  $r_e(B)$  against  $r_e(R)$  for the radio and control galaxies. The  $1\sigma$  errors on  $r_e$ , obtained from the fitting programme, are typically  $\sim 10\%$ . The scale lengths in the two filters are equal to within the  $1\sigma$  in several cases, and these values are scattered around the  $r_e(B) = r_e(R)$  line in the figure. In the other cases we have  $r_e(B) > r_e(R)$  (points below the equality line) or  $r_e(B) < r_e(R)$  (points above). It is obvious from the figure that the latter are more numerous in the radio galaxies, while the former occur more frequently in the control galaxies.

When  $r_e(B) > r_e(R)$ , the surface brightness in  $R$  increases more rapidly towards the center than the surface brightness in  $B$ . In other words, from the definition of the effective radius  $r_e$ , half the red light from the galaxy is contained in a smaller region than half the blue light.  $r_e(B) > r_e(R)$  therefore implies that the galaxy on the average becomes redder inwards. Similarly, when  $r_e(B) < r_e(R)$ , the galaxy becomes bluer as one moves towards the center. The distribution of points in Figure 2 therefore show that the radio galaxies become bluer towards the center more often than the control galaxies.

We have shown in Figure 3 the distribution of the  $r_e(B)/r_e(R)$  ratio in the form of a histogram for both the samples. The distributions are clearly different, with mean values of the ratio for the radio and control samples being  $\langle r_e(B)/r_e(R) \rangle_r = 0.87 \pm 0.15$  and  $\langle r_e(B)/r_e(R) \rangle_c = 1.25 \pm 0.10$ . The larger value of the ratio for the control sample is consistent with previous studies of early type

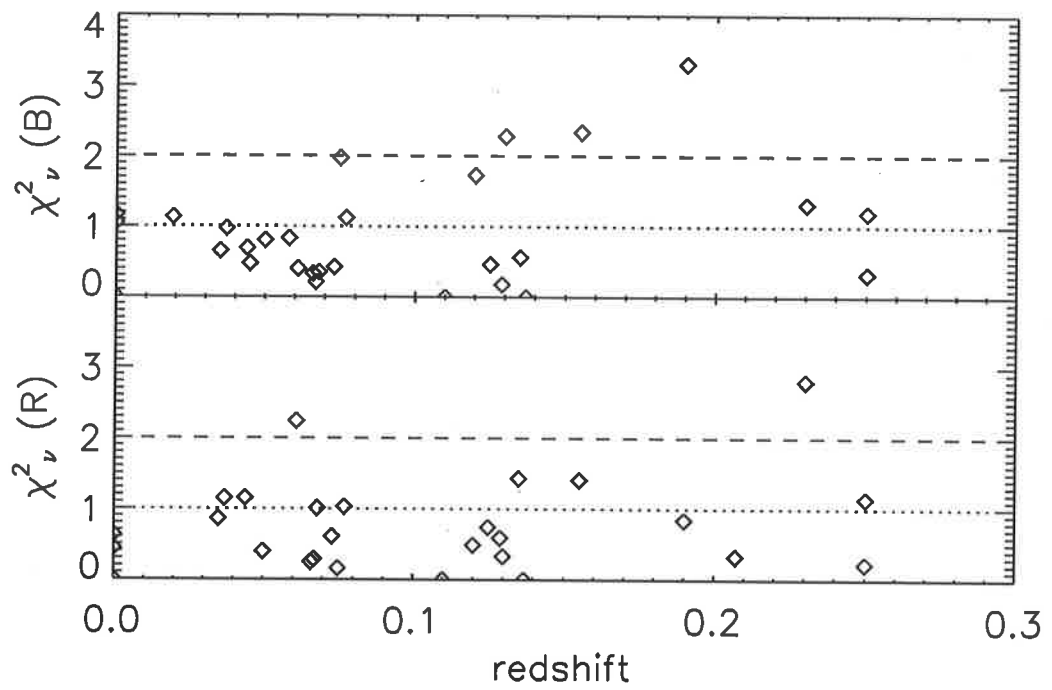


Fig. 1.—  $\chi^2_\nu$  in *B* and *R* filters as a function of redshift.

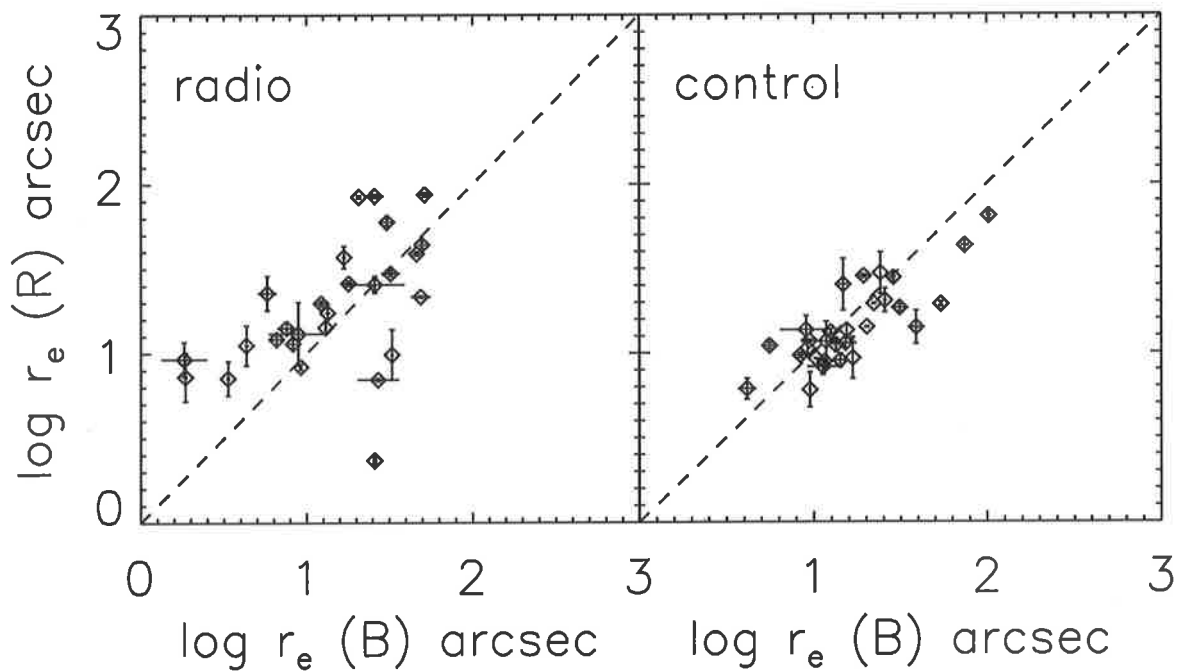


Fig. 2.—  $r_e$  in  $B$  and  $R$  filters for the radio sample (left) and the control sample (right). The dotted line denotes  $r_e(B) = r_e(R)$ . Points above it denote galaxies which become bluer inwards. There is a larger number of such cases amongst the radio galaxies.

galaxies which showed that their colors become redder inwards (e.g. Sandage and Vishwanathan, 1978). Contrary to this behavior, the distribution of the bulge scale length ratio for the radio galaxies shows that they tend to become bluer as one moves towards their inner region. A majority of the radio galaxies become bluer as one approaches the center, i.e., the color variation in radio galaxies is opposite of that in the control galaxies. In the next section we will consider the relation between the scale length ratio and the conventional color gradient.

We have excluded from the profile fits points within 1.5 times the FWHM of the PSF from the center. For our sample the excluded region has a physical dimension extending to  $\sim 4$  kpc at the highest redshift. It follows that the inner bluer color of the radio galaxies is not due to a blue AGN or other unresolved features at the center, and must arise in regions which are quite spread out.

## 5. Color gradients

The color variation in a galaxy is normally measured by a color gradient parameter  $G \equiv \Delta(B - R)/\Delta(\log r)$ . The change in color per decade in radius is almost linear in most galaxies and the color gradient  $G$ , is obtained by fitting a straight line to the color profile between an inner radius  $r_1$  and an outer radius  $r_2$ . We choose these radii as described in Section 3, with the additional caveat that now  $r_2 = \min(r_2(B), r_2(R))$ .

When two small galaxies (angular diameter  $< 15''$ ) and a quasar host in our radio sample are excluded, we find that the mean color gradients, in magnitudes per  $arcsec^2$  per decade in radius, for the radio and control samples are  $\langle G \rangle_r = -0.20 \pm 0.05$  and  $\langle G \rangle_c = -0.23 \pm 0.05$ . The distribution of gradients is shown in Figure 3.

We find that the numbers that we obtain are larger than those obtained by other authors. For a sample of normal ellipticals (with dusty galaxies excluded) Peletier et al. (1990) had obtained a color gradient of  $-0.1$ . Zirbel (1996) had obtained a value of  $-0.15$  for a sample of radio galaxies.

### 5.1. Color gradients and scale length ratios

Color gradients and scale length ratios are both indicative of the change in color with distance from the center and there is a simple relation between them:

$$G \equiv \frac{\Delta(B - R)}{\log r_2/r_1} \simeq \frac{2.06(r_2^{1/4} - r_1^{1/4})}{r_e(B)^{1/4} \log(r_2/r_1)} \left( 1 - \frac{r_e(B)}{r_e(R)} \right), \quad (2)$$

For galaxies that obey de Vaucouleurs' law the color gradient can therefore be obtained from the fitted bulge scale lengths. We enumerate in Table 1 the distribution of color gradients obtained using the scale lengths, as well as the gradients obtained directly from the color profiles using the

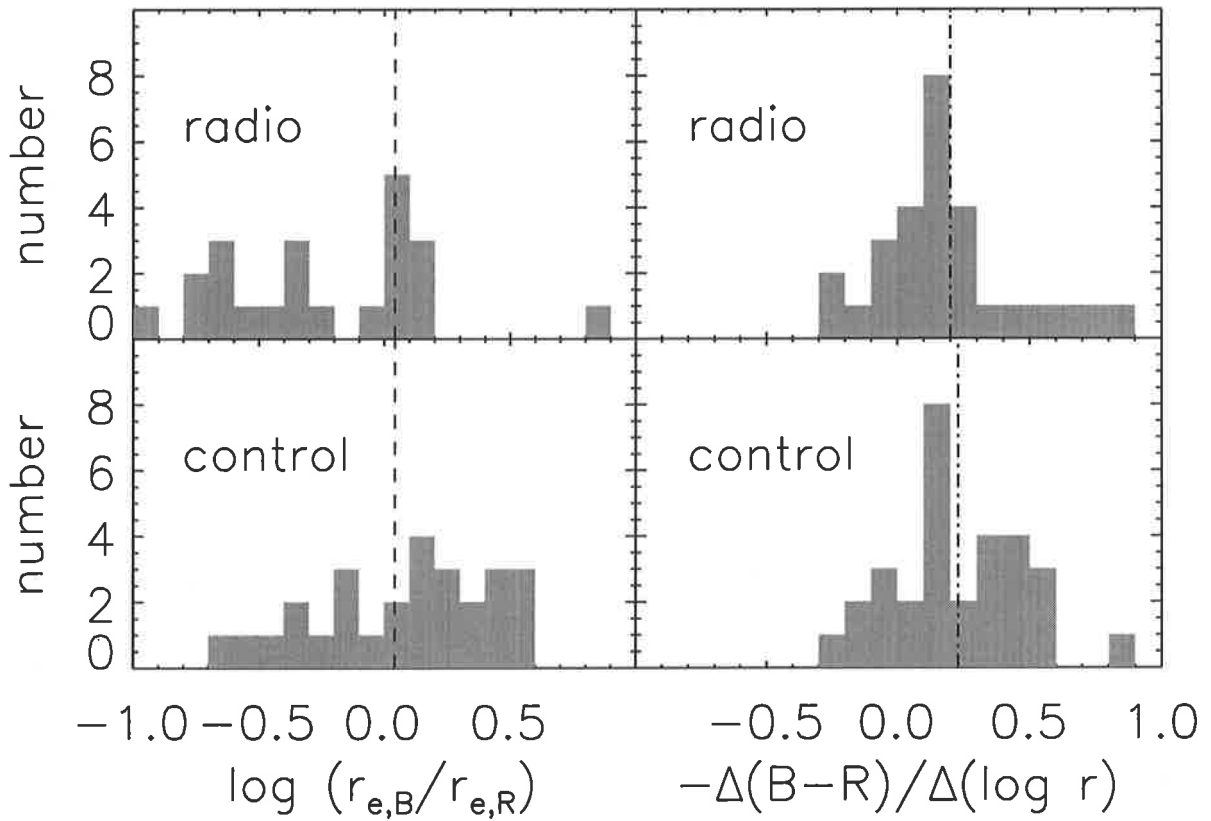


Fig. 3.— The distribution of  $r_e(B)/r_e(R)$  (left) and the color gradient (right) for the radio and control samples. Negative numbers on the x-axis are indicative of galaxies with excess blue emission towards the center.

measured values of the  $B - R$  color at  $r_1$  and  $r_2$ . It is seen from the table that the color gradients obtained directly from the color profiles have a different distribution from the bulge scale length related color gradient. The latter clearly show radio galaxies become bluer towards the center while the control galaxies become redder. This distinction is not obvious from the distribution of the directly measured color gradient.

The conventional color gradient is obtained by fitting a straight line to the color profile, which neglects any curvature that may be present. Also, due to the limited signal-to-noise available, often the errors on the color gradient can be large, making the measured values uncertain. The process of obtaining scale lengths involve averaging over isophotes as well as the profile fit with an empirically tested model. We have seen above that the  $\chi^2_\nu$  obtained are well within acceptable limits in most cases for good fits. The scale lengths are therefore good, robust indicators of the large scale distribution of light in the galaxy, and their ratio in the two filters provides a useful descriptor of the way the color changes over the galaxy. Using the ratio we have demonstrated the ubiquity of inner blue color in radio galaxies, a fact which is not apparent from the conventional color gradient.

## 5.2. Discussion

The color gradient in an early type galaxy is expected mainly to be due to a metallicity gradient mixed with an age gradient (Worthey 1994). But the colors can also be affected by the presence of dust (Wise and Silva 1996), which makes a color redder, or star formation, which makes the color bluer. A galaxy will become bluer towards the inner region either if there is excess star formation towards the center, or if there is excess dust in the outer regions, making them redder relative to the inner region. Dust in the inner regions with a significant covering factor redden the galaxy there.

If we assume that the optical depth of dust is small,  $\tau \ll 1$ , then the extinction produced by

Table 1: Color gradient details for the two samples as obtained from the color profile and from the bulge scale lengths. A negative color gradient is indicative a redder center relative to the outer regions.

Color gradient	From color profile		From scale lengths	
	Radio	Control	Radio	Control
< 0	20	24	9	20
> 0	7	6	18	10
uncertain	3	0	3	0

it is  $\Delta m \simeq 1.06\tau$ . If we further assume that the dust affects only the  $B$  magnitude because of its shorter wavelengths, then the change in color is given by  $\Delta C \equiv \Delta(B - R) \simeq \Delta B \simeq -1.06\tau$ . The color changes due to central dust occur typically over an order of magnitude in distance from the center:  $r_2/r_1 \simeq 10$ . It follows from Equation 2 that the color gradient is  $G \simeq -1.06\tau$ . This corresponds to a scale length ratio of  $r_e(B)/r_e(R) \simeq 1.1$ . In several galaxies with  $r_e(B)/r_e(R) > 1$ , we do find evidence for reddening due to dust in the color maps of the galaxies.

## 6. Extrapolated profiles

In obtaining the best-fit parameters, we have used points along the observed surface brightness profiles which are further from the center than 1.5 times the FWHM of the PSF. The best-fit parameters can be used to generate a model galaxy, and from it the model radial brightness profile obtained after convolution with the PSF. Such a profile can be extrapolated to the center of the galaxy ( $\sim 0''.1$ ) to examine where the observed profile points, close to the center, are situated relative to the model profile.

We find that in some galaxies, the inner points lie within  $1\sigma$  of the extrapolated model profile. This is consistent with de Vaucouleurs' law bulge plus exponential model remaining valid in the innermost region and the absence of significant absorption and emission features. In some case the observed points show an excess over the extrapolation, while in others there is a deficit. Assuming that the model remains valid, the degree of departure is indicative of the amount of excess emission due to star formation or the AGN, while the deficit is indicative of absorption due to dust. If the assumed model does not remain valid, then the departures will have to be modeled before excess emission or absorption can be estimated.

We have shown in Figure 4 the extrapolated profile of the radio galaxy 0520-289, which provides a good example of excess emission. In this case the excess in  $R$  exceeds the excess in  $B$ , which will happen if dust is present and absorbs some of the excess at shorter wavelengths. indicating the presence. The radio galaxy 0446-206 is one of the cases where a deficit is seen, and the color map clearly shows the presence of dust, showing that much of the deficit is indeed likely to be due to absorption.

We have quantified the excess emission and the absorption due to dust by accumulating the difference between the model galaxy profile and the observed surface brightness profile in the inner region. The total excess is then given by the ratio of the cumulative sum to the luminosity of de Vaucouleurs bulge. Absorption due to dust is indicated by a negative excess. We find that the excess for the control sample galaxies is over an order of magnitude smaller than that for the radio galaxies.

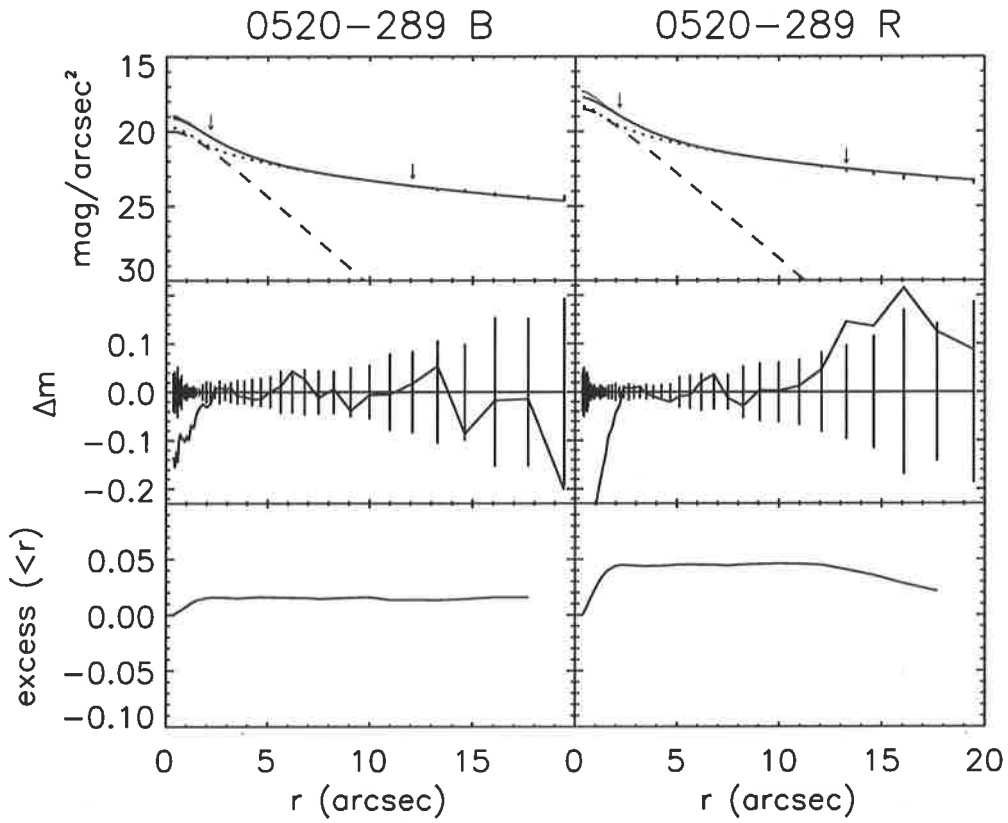


Fig. 4.— The radio galaxy 0520-289 which shows excess emission near the center.  $B$  and  $R$  profile fits are shown in the left and right columns respectively. The panels at the top depict the observed profile (points), the model bulge component (dotted line), disk component (dashed line) and their sum (solid line). The disk has a sub-PSF scale length and  $D/B = 0.14$  in both the filters. The middle panels shows the residual surface magnitude  $\Delta m = m_{observed} - m_{fit}$ , along with error bars on the observed profile. The bottom panels show the fractional cumulative excess upto a semi-major axis length  $r$  as a function of  $r$ .

## 7. Conclusions

Using detailed model profile fits to the observed surface brightness profiles of samples or radio and control galaxies, we have shown that the distribution of the  $r_e(B)/r_e(R)$  ratio is different for the two samples. A value  $< 1$  for this ratio in a galaxy indicates that the color of the galaxy becomes bluer towards the center, while  $r_e(B)/r_e(R) > 1$  indicates that the color becomes redder towards the center. The ratio has a simple relation with the color gradient  $G$  obtained directly from color profiles. But the ratio can be used as an indicator of the radial dependence of color, even when the measured gradient is too noisy to serve the purpose. Extrapolation of model profiles to inner regions, which are not used in the fit, provide a measure of star formation activity and dust absorption near the center.

## REFERENCES

- Jedrzejewski R. I. 1987, MNRAS, 226, 747  
Mahabal A., et al. 1998a, (in preparation)  
Mahabal A., et al. 1998b, (in preparation)  
Peletier R. F., et al. 1990, AJ, 100, 1091  
Sandage A., & Vishwanathan N. 1978, ApJ, 223, 707  
Smith E. P., & Heckman T. M. 1989, ApJ, 341, 658  
Wise M. W., & Silva D. R. 1996, ApJ, 461, 155  
Worthey G. 1994, ApJS, 95, 107  
Zirbel E. 1996, ApJ, 473, 713